



## Synthesis and vibrational study of phosphate-sulfate fluorapatites

### $\text{Ca}_{10-x}\text{Na}_x(\text{PO}_4)_6-x(\text{SO}_4)_x\text{F}_2$ ( $0 \leq x \leq 6$ )

Faten Nouri<sup>a\*</sup>, Gérard Panczer<sup>b</sup>, Malika Trabelsi-Ayadi<sup>a</sup>, Riadh Ternane<sup>a\*</sup>

<sup>a</sup>Laboratoire d'Application de la Chimie aux Ressources et Substances Naturelles et à l'Environnement (LACReSNE), Université de Carthage, Faculté des Sciences de Bizerte, 7021 Zarzouna, Bizerte, Tunisia

<sup>b</sup>Institut Lumière Matière, UMR-CNRS 5306, Université Lyon1, F-69622 Villeurbanne Cedex, France

Faten Nouri  
nourifeten@gmail.com  
Riadh Ternane  
rternane@yahoo.fr

### ABSTRACT

A series of phosphate-sulfate fluorapatites  $\text{Ca}_{10-x}\text{Na}_x(\text{SO}_4)_x(\text{PO}_4)_{6-x}\text{F}_2$  has been synthesized by the solid-state reaction at high temperature. The samples were characterized using X-ray diffraction, Infrared spectroscopy and Raman scattering spectroscopy. X-ray diffraction study shows that these materials crystallize in the hexagonal system with  $\text{P6}_3/\text{m}$  as space group. Infrared and Raman spectra are reported and band assignments are made.

### Keywords

Sulfate fluorapatite, X-ray diffraction, Infrared absorption, Raman scattering spectroscopy.

### Academic Discipline And Sub-Disciplines

Chemistry

### SUBJECT CLASSIFICATION

Chemistry subject classification

### TYPE (METHOD/APPROACH)

Experimental study

## 1. INTRODUCTION

Apatites are solid inorganic compounds, represented by the general formula  $\text{Me}_{10}(\text{XO}_4)_6\text{A}_2$ , they crystallize in the hexagonal system with the space group  $\text{P6}_3/\text{m}$  [1]. The apatite structure provides a great capacity to form solid solutions and, particularly, to accept several substitutes for example, the monovalent A ion can be  $\text{OH}^-$ ,  $\text{F}^-$ ,  $\text{O}^{2-}$ ,  $\text{CO}_3^{2-}$ ..., the trivalent anion  $\text{XO}_4$  can be  $\text{AsO}_4^{3-}$ ,  $\text{VO}_4^{3-}$ ,  $\text{CrO}_4^{3-}$ ,  $\text{HPO}_4^{2-}$ ,  $\text{CO}_3^{2-}$ ,  $\text{SO}_4^{2-}$ ,  $\text{SiO}_4^{4-}$ . There is no literature information showing that vacancies could exist on the ( $\text{XO}_4$ ) site. Me cations may be divalent ( $\text{Ca}^{2+}$ ,  $\text{Ba}^{2+}$ ,  $\text{Pb}^{2+}$ ) monovalent ( $\text{Na}^+$ ) or even trivalent (Rare Earth Element  $\text{REE}^{3+}$ ). The apatite-like structure is characterized by the presence of two types of tunnels permitting the location of two cationic sites labeled Me(I) and Me(II): four Me(I) are at the centre of narrow tunnels (4f sites), six Me(II) around large tunnels (6h sites). The coordination number of Me (I) and Me(II) sites are nine and seven, respectively. However, extensive substitutions can occur on the different cation and anion sites in mineral samples.

Since the P-O and S-O bond distances in the corresponding  $\text{PO}_4^{3-}$  and  $\text{SO}_4^{2-}$  tetrahedral are similar (P-O: 1.50 Å, S-O: 1.44 Å) [2-3]. Up to now the group of sulfate apatite has not been studied in such details. Sulfate apatite can be derived from phosphate apatite by coupled substitution of  $\text{PO}_4^{3-}$  and  $\text{Ca}^{2+}$  with  $\text{SO}_4^{2-}$  and  $\text{Na}^+$  [4]. Furthermore, phosphate-sulfate apatites, were found to have some interesting properties [5-7]. Mixed phosphate-sulfate fluorapatites have been investigated by Laghzizil et al. [8] and Piotrowski et al. [9]. They indicate that samples synthesized by solid state reactions usually consist of the two end members  $\text{Ca}_4\text{Na}_6(\text{SO}_4)_6\text{F}_2$  and  $\text{Ca}_{10}(\text{PO}_4)_6\text{F}_2$ . Up to now, the vibrational study (IR and Raman) of the phosphate-sulfate fluorapatites has not been studied.

In this work, the fluorapatites  $\text{Ca}_{10-x}\text{Na}_x(\text{PO}_4)_{6-x}(\text{SO}_4)_x\text{F}_2$  ( $0 \leq x \leq 6$ ) have been prepared by solid state reaction. The structural characterization of the prepared materials has been performed with XRD, FTIR and Raman techniques.

## 2. EXPERIMENTAL

### 2.1. Synthesis

Five samples with formula  $\text{Ca}_{10}(\text{PO}_4)_6\text{F}_2$ ,  $\text{Ca}_9\text{Na}(\text{PO}_4)_5(\text{SO}_4)\text{F}_2$ ,  $\text{Ca}_7\text{Na}_3(\text{PO}_4)_3(\text{SO}_4)_3\text{F}_2$ ,  $\text{Ca}_5\text{Na}_5(\text{PO}_4)(\text{SO}_4)_5\text{F}_2$  and  $\text{Ca}_4\text{Na}_6(\text{SO}_4)_6\text{F}_2$  symbolized by FS0P6, FS1P5, FS3P3, FS5P1 and FS6P0, respectively, have been synthesized by solid-state reaction. The temperature varies between 773 K, 823 K and 1173 K depending on the S/P ratio.

The compounds were prepared by an initial mixture of sodium sulfate  $\text{Na}_2\text{SO}_4$ , calcium carbonate  $\text{CaCO}_3$ , calcium fluoride  $\text{CaF}_2$ , di-ammonium hydrogen phosphate  $(\text{NH}_4)_2\text{HPO}_4$  and di-ammonium sulfate  $(\text{NH}_4)_2\text{SO}_4$ , with the atomic ratio  $\text{Ca}+\text{Na}/\text{S}+\text{P}$  fixed at 1.667. Stoichiometric amounts of reactants have been ground and heated in covered platinum

crucibles at 773 K for 72h, then at 823 K for 24 h, and at 1173 K for 72h. The heat treatment was accompanied by several grindings in order to get well-crystallized products.

### 2.1.1. Experimental techniques

The samples were identified by X-ray diffraction (XRD) patterns recorded with a Bruker D8-advance diffractometer using CuK $\alpha$  radiation ( $\lambda=1.5406\text{\AA}$ ). X-ray diffraction data have been collected over the  $10^\circ\text{-}55^\circ$   $2\theta$  range. The crystalline phases have been identified using the International Centre for Diffraction Data (ICDD) powder diffraction files. The unit cell parameters values were calculated using the «FullProf» program.

IR spectra were recorded using a Fourier Transform Infrared spectrometer with an attenuated total reflectance accessory (FTIR-ATR). The FTIR-ATR Perkin Elmer Spectra 100 spectrometer was equipped with a diamond ATR universal system and the spectral range spans from  $400$  to  $1700\text{ cm}^{-1}$  with a  $2\text{ cm}^{-1}$  spectral resolution.

Raman spectra were recorded using an Aramis Horiba Jobin-Yvon spectrometer at 473nm laser excitation (Helium-Neon); grating 1800/mm, spectral resolution  $0.52\text{ cm}^{-1}$ . The spot diameter for a x50 (0.55 NA) objective is  $1.4\mu\text{m}$ ; photo detector cooling CCD, with an exposition of 5s of acquisition and 10 accumulations.

## 3. RESULTS AND DISCUSSION

### 3.1. X- ray diffraction

Powder XRD patterns of prepared FS6P0, FS5P1, FS3P3, FS1P5 and FS0P6 compounds correspond to well crystallized phases. XRD patterns have been fitted with the hexagonal unit cell (S.G.P6 $_3$ /m). XRD patterns have showed that all prepared samples are single phases displaying the apatite structure (Fig. 1). Crystal data deduced from XRD analysis are given in Table1.

The variations of the a and c unit cell parameters are given in Fig.2, The decrease of a and c parameters is attributed to the substitution of PO $_4^{3-}$  and Ca $^{2+}$  ions by smaller SO $_4^{2-}$  and Na $^+$  ions (P $^{5+}$  (0.17 Å), Ca $^{2+}$  (1.00 Å), S $^{6+}$  (0.12 Å), Na $^+$  (1.02 Å)) [10]. Moreover, the continuous evolutions of a and c parameters follow the Vegard'slaw. This indicates the occurrence of a continuous solid solution inside the defined single-phase domain of phosphate-sulfate fluorapatites.

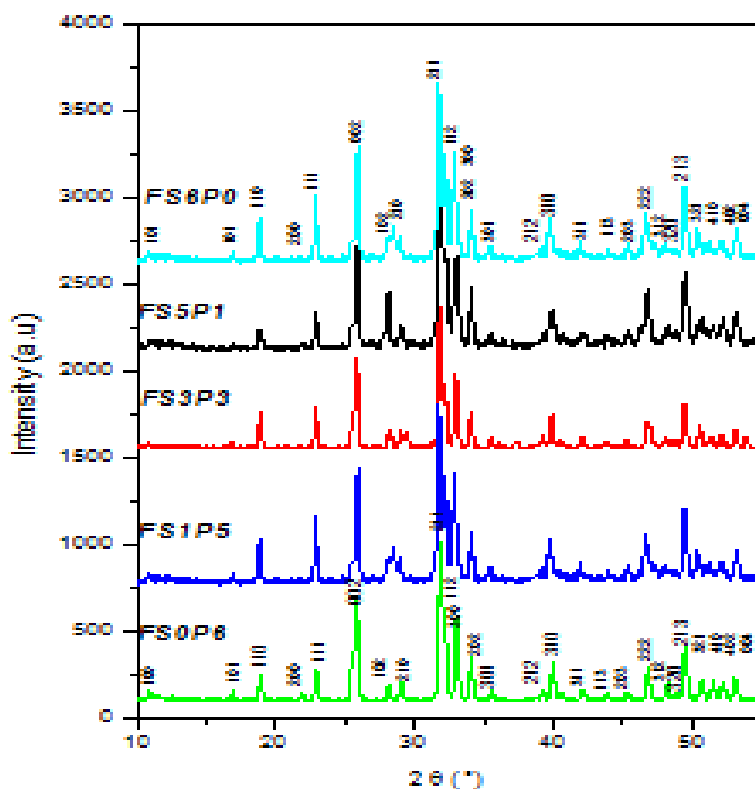


**Figure 1:** X-ray diffraction patterns of Ca $_{10-x}$ Na $_x$ (PO $_4$ ) $_{6-x}$ (SO $_4$ ) $_x$ F $_2$  fluorapatites (from FS0P6 to FS6P0)



**Table 1:** Unit-cell parameters of  $\text{Ca}_{10-x}\text{Na}_x(\text{PO}_4)_{6-x}(\text{SO}_4)_x\text{F}_2$  fluorapatites

Compound	FS0P6	FS1P5	FS3P3	FS5P1	FS6P0
a (Å)	9.381(1)	9.374(3)	9.360(7)	9.347(1)	9.340(6)
c (Å)	6.875(3)	6.871(0)	6.864(6)	6.857(8)	6.853 (4)
V(Å <sup>3</sup> )	528.751	528.440	527.801	527.100	526.749
Crystal system	Hexagonal				
Space group	P6 <sub>3</sub> /m				

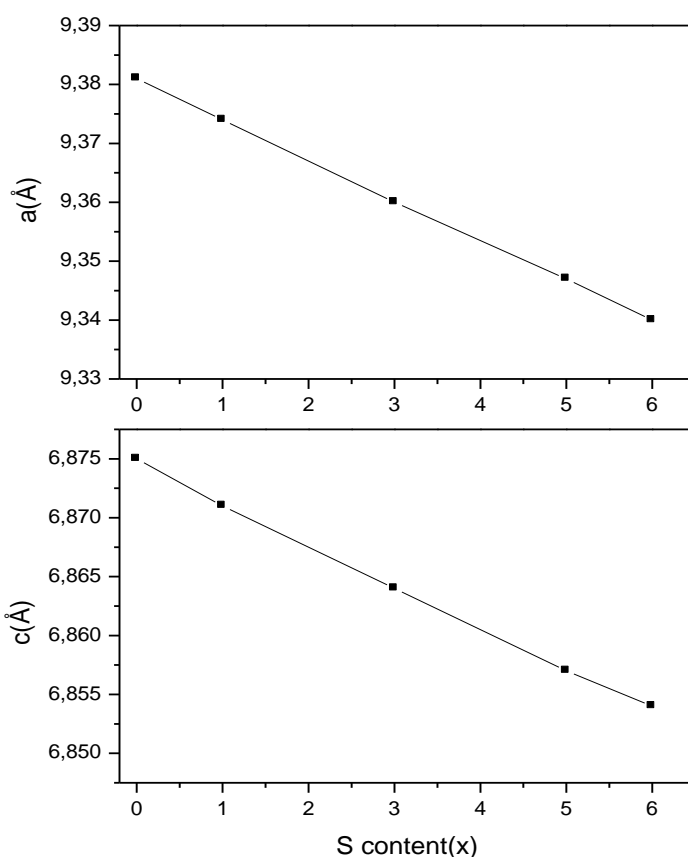


**Figure 2:** Variation of a and c unit cell parameters versus S content(x) of  $\text{Ca}_{10-x}\text{Na}_x(\text{PO}_4)_{6-x}(\text{SO}_4)_x\text{F}_2$  fluorapatites

## 3.2. Vibrational spectroscopy

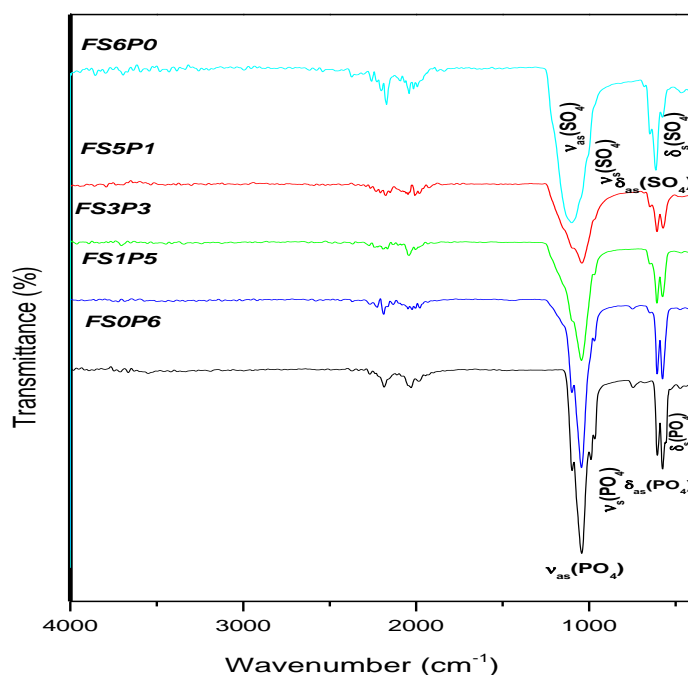
### 3.2.1. Infrared spectra

Fig. 3 shows the infrared (IR) spectra of the  $\text{Ca}_{10-x}\text{Na}_x(\text{PO}_4)_{6-x}(\text{SO}_4)_x\text{F}_2$  fluorapatites in the 4000-400  $\text{cm}^{-1}$  range. The band assignment is given in Table 2. The assignment of IR bands of fluorapatites has been performed according to published literature [11,15]. IR spectra displayed absorption bands between 1129 and 1004  $\text{cm}^{-1}$  (symmetric  $\nu_s$  and antisymmetric  $\nu_{as}$  stretching vibrations) and relatively sharp bands between 650 and 400  $\text{cm}^{-1}$  (symmetric  $\delta_s$  and antisymmetric  $\delta_{as}$  bending vibrations) due to isolated  $\text{XO}_4$  tetrahedra (X = P, S).

The IR spectrum of the FS6P0 shows four ranges of absorption between 1129-1105, 1004, 650-607 and 487-472  $\text{cm}^{-1}$ . The bands corresponding to the first range are assigned to antisymmetric stretching vibrations  $\nu_{as}(\text{SO}_4)$  at 1105-1129  $\text{cm}^{-1}$ . The band at 1004  $\text{cm}^{-1}$  is attributed to symmetric stretching vibrations  $\nu_s(\text{SO}_4)$ . The bands at 650-607 and 472-487  $\text{cm}^{-1}$  are assigned to the antisymmetric  $\delta_{as}(\text{SO}_4)$  and the symmetric  $\delta_s(\text{SO}_4)$  bending vibrations, respectively.

For the FS0P6 sample, one can note the presence of the bands assigned to PO<sub>4</sub> groups. There are six bands of internal modes instead of the nine factor group expected for active modes. The bands at 1040-1097 cm<sup>-1</sup> and 964 cm<sup>-1</sup> are attributed to the antisymmetric stretching  $\nu_{as}(\text{PO}_4)$  and the symmetric stretching  $\nu_s(\text{PO}_4)$  modes of the PO<sub>4</sub> groups, respectively. The vibrations at 574-605 and 433-474 cm<sup>-1</sup> are attributed to the antisymmetric  $\delta_{as}(\text{PO}_4)$  and the symmetric  $\delta_s(\text{PO}_4)$  bending vibrations, respectively.

The spectra of FS3P3, FS1P5 and FS5P1 samples are dominated by two groups of bands. A first group of bands located between 572 and 605 cm<sup>-1</sup> attributed to  $\delta_{as}(\text{PO}_4)$ , 607-649 cm<sup>-1</sup> attributed to  $\delta_{as}(\text{SO}_4)$  in the apatitic structure. The bands located at 1041-1082 cm<sup>-1</sup> are attributed to the  $\nu_{as}(\text{PO}_4)$  vibrations, 1105 and 1129 cm<sup>-1</sup> are attributed to the  $\nu_{as}(\text{SO}_4)$  vibrations in the apatitic structure. The shoulder situated at 433-474 cm<sup>-1</sup> are assigned by the  $\delta_s(\text{PO}_4)$  mode, 470 cm<sup>-1</sup> is assigned by the  $\delta_s(\text{SO}_4)$  mode while the band situated at 964 cm<sup>-1</sup> is attributed to the  $\nu_s(\text{PO}_4)$ , 1004 cm<sup>-1</sup> is attributed to the  $\nu_s(\text{SO}_4)$  in the apatitic structure. These bands shift progressively toward higher wavenumbers with the increase of S content (x) (Fig. 3). The absence of the bands due to OH<sup>-</sup> (3572 cm<sup>-1</sup>), CO<sub>3</sub><sup>2-</sup> (1410-1450, 860-885 cm<sup>-1</sup>) and HPO<sub>4</sub><sup>2-</sup> (1180-1200, 875 cm<sup>-1</sup>) ions indicates the absence of appreciable amounts of impurities [12-14]. The broadening of the IR bands with increasing the S content (x) is explained by the substitution effect. These results confirm the purity of the investigated samples.



**Figure 3:** FTIR spectra of Ca<sub>10-x</sub>Na<sub>x</sub>(PO<sub>4</sub>)<sub>6-x</sub>(SO<sub>4</sub>)<sub>x</sub>F<sub>2</sub> fluorapatites (from FS0P6 to FS6P0)

### 3.2.2. Raman scattering

Fig. 4 shows the Raman spectra of the Ca<sub>10-x</sub>Na<sub>x</sub>(PO<sub>4</sub>)<sub>6-x</sub>(SO<sub>4</sub>)<sub>x</sub>F<sub>2</sub> fluorapatites in the

200-1200 cm<sup>-1</sup> range. The band assignment is given in Table 2. The observed band positions can be assigned to their corresponding modes based on the related fluorapatites in literature [15-17]. In theory, the sulfate group is characterized by six bands Raman, which include three stretching modes (1 $\nu_s$ (SO<sub>4</sub>) and 2 $\nu_{as}$ (SO<sub>4</sub>)) and three bending modes (1 $\delta_s$ (SO<sub>4</sub>) and 2 $\delta_{as}$ (SO<sub>4</sub>)) [18-22].

The FS6P0 spectrum presents a band of high intensity at 1105-1129 cm<sup>-1</sup> attributed to  $\nu_{as}$  vibration mode (SO<sub>4</sub>). The other band at 1004 cm<sup>-1</sup> is assigned to  $\nu_s$  vibration mode. The three bands are attributed to the  $\delta_{as}(\text{SO}_4)$  and the  $\delta_s(\text{SO}_4)$  modes.

The FS0P6 spectrum is dominated by two groups of bands. A first group of bands located between 580 and 605 cm<sup>-1</sup> is attributed to  $\delta_{as}(\text{PO}_4)$  in the apatitic structure. The bands located at 1041-1053 and 1087 cm<sup>-1</sup> are attributed to the  $\nu_{as}(\text{PO}_4)$  vibrations in the apatitic structure. The shoulder situated at 430-445 cm<sup>-1</sup> is assigned by the  $\delta_s(\text{PO}_4)$  mode while the band situated at 966 cm<sup>-1</sup> is attributed to the  $\nu_s(\text{PO}_4)$  in the apatitic structure.

The spectra of FS1P5, FS5P1 and FS3P3 consist of a mixture of two apatite end-members FS0P6 and FS6P0.

The Raman bands shift progressively toward higher wavenumbers with the increase of S content (x) (Fig. 4).



According to these results, some interesting remarks can be deduced: 1) the Raman spectra do not exhibit a band at  $850\text{ cm}^{-1}$  attributed to peroxide ( $\text{O}_2^{2-}$ ) anions in apatites [23], 2) the absence of bands at  $3572$  and  $630\text{ cm}^{-1}$ , corresponding to stretching and libration modes of OH groups, proves that synthesized samples are not hydroxyapatites [14].

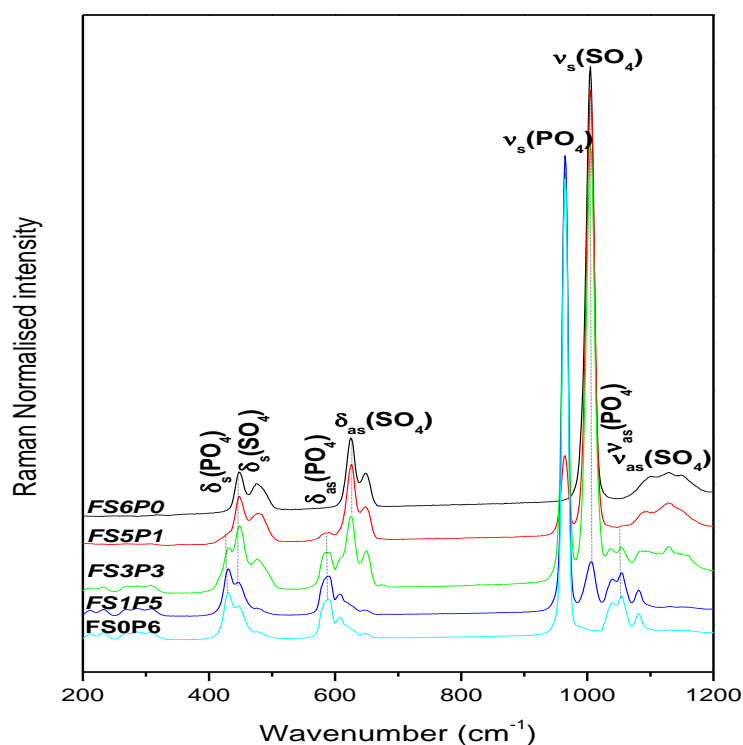


**Figure 4:** Raman spectra of  $\text{Ca}_{10-x}\text{Na}_x(\text{PO}_4)_{6-x}(\text{SO}_4)_x\text{F}_2$  fluorapatites (from FS0P6 to FS6P0)

**Table 2:** Assignments ( $\text{cm}^{-1}$ ) of FT-IR and Raman spectra of  $\text{Ca}_{10-x}\text{Na}_x(\text{PO}_4)_{6-x}(\text{SO}_4)_x\text{F}_2$  fluorapatites

Compound	Infrared spectroscopy				Raman spectroscopy			
	$\nu_s$	$\bar{\nu}_s$	$\nu_{as}$	$\bar{\nu}_{as}$	$\nu_s$	$\bar{\nu}_s$	$\nu_{as}$	$\bar{\nu}_{as}$
FS0P6	964	474-433	1097-1040	605-574	966	445-430	1087-1053-1041	605-580
FS1P5	-	-	1129-1105( $\text{SO}_4$ )	-	1004( $\text{SO}_4$ )	-	-	-
	964 ( $\text{PO}_4$ )	-	1039 ( $\text{PO}_4$ )	605- 570( $\text{PO}_4$ )	964( $\text{PO}_4$ )	445-430( $\text{PO}_4$ )	1080-1056-1040( $\text{PO}_4$ )	605( $\text{PO}_4$ )
FS3P3	1004( $\text{SO}_4$ )	470 ( $\text{SO}_4$ )	1105( $\text{SO}_4$ )	649-607( $\text{SO}_4$ )	1004( $\text{SO}_4$ )	447( $\text{SO}_4$ )	1129-1105( $\text{SO}_4$ )	649-626( $\text{SO}_4$ )
	964( $\text{PO}_4$ )	433( $\text{PO}_4$ )	1082-1041( $\text{PO}_4$ )	605-572( $\text{PO}_4$ )	964( $\text{PO}_4$ )	430( $\text{PO}_4$ )	1080-1052-1037( $\text{PO}_4$ )	587( $\text{PO}_4$ )
FS5P1	-	470( $\text{SO}_4$ )	1105( $\text{SO}_4$ )	650( $\text{SO}_4$ )	1004( $\text{SO}_4$ )	478-447( $\text{SO}_4$ )	1129( $\text{SO}_4$ )	649-626( $\text{SO}_4$ )
	964( $\text{PO}_4$ )	433( $\text{PO}_4$ )	1040( $\text{PO}_4$ )	574-605( $\text{PO}_4$ )	964( $\text{PO}_4$ )	430 ( $\text{PO}_4$ )	1085-1050( $\text{PO}_4$ )	588 ( $\text{PO}_4$ )
FS6P0	1004	487-472	1129-1105	650-607	1004	479-450	1129-1105	649 -607

## 4. CONCLUSION



The present work deals with the synthesis and the characterization of the

$\text{Ca}_{10-x}\text{Na}_x(\text{PO}_4)_{6-x}(\text{SO}_4)_x\text{F}_2$  ( $0 \leq x \leq 6$ ) fluorapatites using XRD, Raman and FTIR spectroscopies. XRD patterns confirmed the formation of single apatite phase. The spectroscopic study (IR and Raman) has made it possible to define more precisely the assignment of the different bands. In the IR and Raman spectra, the relative intensity of the bands assigned to  $\text{PO}_4$  and  $\text{SO}_4$  groups agrees with the change of S/P ratio. The band wavenumbers of the vibrations assigned to  $\text{XO}_4$  groups ( $\text{X}=\text{P}, \text{S}$ ) shift to higher values significantly with the decrease in the size of the ion.

## References

- [1] Prener J.S., *J. Solid State Chem.* 3 (1971) 49.
- [2] Prince E., *J. Int. T. Crystallogr.* 2004.
- [3] Botta C., Kahlenberg V., Hejny C., Többens D. M., M Bykov. and Van Smaalen S., *J. Miner. Petrol.* 108 (2014) 487.
- [4] Klement R., *Naturwissenschaften.* 27 (1939) 568.
- [5] A Piotrowski., Kahlenberg V., Lee Y., Parise J. B., R.X. Fischer. *J. Mineral.* 87 (2002) 715.
- [6] Anton R., John M. *J. Mineral.* 43 (2005) 735.
- [7] Tonsuaadu K., Peld M., Quarton M., Bender V., Veiderma M., *J. Oganometall. Chem.* 177 (2002) 1873.
- [8] Laghzizil A., El Hajjaji S., Bouhaouss A., Ferhat M. *Solid State Ionics.* 126 (1999) 245.
- [9] Piotrowski A., Kahlenberg V., R.X.Fischer. *J. Mineral* 16 (2004) 279.
- [10] Shannon R. D., *Acta Crystallogr* 32 (1976) 751.
- [11] Toyama T., Kameda S., Nishimiya N. *Bioceram. Dev. Appl.* 2090 (2013) 5025.
- [12] Hughes J. M., Cameron M., Crowley K. D., *Amer. Min.* 74 (1989) 870.
- [13] Ntahomvukiye I., Khattech I., Jemal M. *Ann. Chim. Fr* 1 (1995) 20.
- [14] Arends J., Christoffersen J., Christoffersen M. R., Eckert H., Fowler B.O., Heughebaert J.C., Nancollas G.H., Yesinowski J.P., Zawacki S.J. *J. Cryst. Growth* 84 (1987) 515.
- [15] Apella M. C., Baran E. J., *Spectrosc. Lett* 1 (1979) 12.
- [16] Kolitsch U., Tiekink E. R. T., Slade P. G., Taylor M. R., Pring A. *Eur. J. Mineral* 11 (1999) 513.
- [17] Maubec N., Lahfid A., C Lerouge., Wille G., Michel K. *Spectrochim. Acta* 96 (2012) 925.
- [18] Frost R. L., Palmer, S. *J. Mol. Struct* 994 (2011) 232.
- [19] Toumi M., Tlili A. *J. Inorg. Chem.* 53 (2008) 1845.
- [20] Breitinger D. K., Kriegelstein R., Bogner A., Schwab R. G., Pimpl T. H., Mohr J., Schukow H. *J. Mol. Struct.* 408 (1997) 287.
- [21] Frost R. L., Wills R. A., Weier M. L., Martens W., Kloprogge J. T. *J. Mol. Struct.* 785 (2006) 123.
- [22] Rudolph W.W., Mason R.J. *Solution Chem.* 30 (2001) 527.
- [23] Trombe J.C. *Ann. Chim.* 8 (1973) 335.